
MITIGATING THE INFLUENCE OF DOMAIN SHIFT IN SKIN LESION CLASSIFICATION: A BENCHMARK STUDY OF UNSUPERVISED DOMAIN ADAPTATION METHODS ON DERMOSCOPIC IMAGES

PREPRINT

Sireesha Chamarthi*

Data Analysis and Intelligence
German Aerospace Center (DLR)
Jena, Germany
Sireesha.Chamarthi@dlr.de

Katharina Fogelberg*

Digital Biomarkers for Oncology
German Cancer Research Center (DKFZ)
Heidelberg, Germany
katharina.fogelberg@dkfz-heidelberg.de

Roman C. Maron

Digital Biomarkers for Oncology
German Cancer Research Center (DKFZ)

Titus J. Brinker

Digital Biomarkers for Oncology
German Cancer Research Center (DKFZ)

Julia Niebling

Data Analysis and Intelligence
German Aerospace Center (DLR)

ABSTRACT

The potential of deep neural networks in skin lesion classification has already been demonstrated to be on-par if not superior to the dermatologists' diagnosis. However, the performance of these models usually deteriorates when the test data differs significantly from the training data (i.e. domain shift). This concerning limitation for models intended to be used in real-world skin lesion classification tasks poses a risk to patients. For example, different image acquisition systems or previously unseen anatomical sites on the patient can suffice to cause such domain shifts. Mitigating the negative effect of such shifts is therefore crucial, but developing effective methods to address domain shift has proven to be challenging. In this study, we carry out an in-depth analysis of eight different unsupervised domain adaptation methods to analyze their effectiveness in improving generalization for dermoscopic datasets. To ensure robustness of our findings, we test each method on a total of ten distinct datasets, thereby covering a variety of possible domain shifts. In addition, we investigated which factors in the domain shifted datasets have an impact on the effectiveness of domain adaptation methods. Our findings show that all of the eight domain adaptation methods result in improved AUPRC for the majority of analyzed datasets. Altogether, these results indicate that unsupervised domain adaptations generally lead to performance improvements for the binary melanoma-nevus classification task regardless of the nature of the domain shift. However, small or heavily imbalanced datasets lead to a reduced conformity of the results due to the influence of these factors on the methods' performance.

Keywords domain shift · skin lesion classification · dermoscopic image · unsupervised domain adaptation · generalization

*Both authors contributed equally

1 Introduction

Deep Neural Networks (DNNs) transformed machine learning by significantly improving predictive accuracy, even in complex real-world applications like skin cancer classification. Usually, DNNs are trained on large datasets, so they learn the representations effectively. Apart from that, the training dataset (or source) and the test dataset (or target) for classification models are drawn from the same distribution. However, in skin cancer classification, as well as in other real-world scenarios, the source and target domains are generally different. Even a small-scale deviation from the distribution of the training domain can result in unreliable and deteriorated predictions on the target domain Yosinski et al. [2014], Ovadia et al. [2019], Tzeng et al. [2017], Xu et al. [2019]. This deviation between datasets is commonly referred to as domain shift. In dermatology, these domain shifts can be caused by a combination of different factors, such as changes in the settings of an image acquisition system, view angle, lighting conditions in the examination room or the way the dermatoscope is positioned, among others.

As such domain shifts lead to a drop in performance, there exist different approaches to handle that problem, e.g. data augmentation Yao et al. [2022], domain generalization Wang et al. [2021] and domain adaptation (DA) Wang and Deng [2018], Guo et al. [2021]. Domain generalization and DA are closely related. While domain generalization methods do not access any data from the target domain, domain adaptation methods may make use of data from the target domain by definition. Nevertheless, all these approaches can only reduce, but not remove the discrepancy between domains Yosinski et al. [2014].

Domain adaptation is typically applied in cases where the domain feature spaces and tasks remain the same while only the distributions differ between source and target datasets (presence of a domain shift) Quinero-Candela et al. [2008], Long et al. [2015], Ganin and Lempitsky [2015]. Mainly this is done by either moment-matching methods or by adversarial learning Long et al. [2018]. The knowledge transfer from source to target works via finding domain-invariant representations, which are used to bridge the discrepancy between domains Pan and Yang [2010].

Unsupervised Domain Adaptation (UDA) methods are well studied and established on multiple benchmark datasets (usually natural images), like Office-10, Caltech-10, Office-31, MNIST and SVHN datasets [Patel et al., 2015, Wang and Deng, 2018, Zhang, 2021], but their performance is not verified on new tasks Jin et al. [2020]. Therefore it may be more difficult to choose a proper method for real-life applications. Apart from this, existing medical images are mostly unlabeled as it is generally difficult to obtain labeled data in the medical field. For a sufficient ground truth (labels) for dermoscopic images, a biopsy of the human lesion needs to be performed. Therefore, the overall process of obtaining and reliably labeling dermoscopic data is labor-intensive. That is why further task-specific fine-tuning of DNN is time-consuming and difficult. These limitations can be addressed by utilizing specifically domain adaptation methods which are unsupervised [Guan and Liu, 2022].

To our knowledge, there is no previous research that applies UDA methods as a benchmark on dermoscopic skin cancer datasets. Most existing works on domain adaptation assume their datasets to be domain shifted without quantifying it. However, in more complex tasks such as dermoscopic image classification, where even medical experts struggle to differentiate melanomas and nevi in particular situations, it is crucial to ensure that the datasets are truly domain shifted. In our previous work Fogelberg et al. [2023], we grouped and quantified domain shifted datasets for dermoscopic skin cancer classification, which we will use in this study. Additionally, other studies acknowledge their performance improvements without focusing on influential factors. However, we aim to identify possible factors for this performance improvement. Furthermore, other studies typically focus only on their benchmark and do not compare their results to other tasks, which can limit the generalizability of their findings. Therefore, while good performance on one method with one dataset or task may indicate its effectiveness, it does not guarantee the same performance improvement with other datasets or tasks.

Our contributions are the following:

- we provide a comparative analysis of 8 UDA methods on 11 dermoscopic datasets with quantified (not assumed) biological and technical domain shifts.
- we identify dataset-specific factors on the performance of UDA methods.
- we compare our results to other benchmark domain adaptation datasets (e.g. Office-31).

This work is structured as follows: First we discuss related works which focuses on UDA methods and benchmarking in Section 2. In Section 3 we describe the used dermoscopic datasets and the UDA methods we compared in our analyses. We further explain our experimental settings. Finally, in Section 4 we explain our results regarding different aspects of comparison. We discuss the influence of class imbalance, target dataset size, as well as the performance itself using the Area Under the Receiver Operating Characteristic (AUROC) and the Area Under the Precision-Recall Curve (AUPRC). We conclude the paper in Section 5 with our findings and discuss possible future research directions.

2 Related work

Ben-David et al., Ben-David et al. [2009] pioneered domain adaptation theory and further classified DA methods to supervised and unsupervised approaches based on label availability. In Supervised Domain Adaptation (SDA) the model is trained on the source domain and tested on the target domain, both with labeled data. The most common approach for SDA is pretraining on the source domain and fine-tuning on the target domain. However, for the translation of medical applications into the clinic this approach is impractical and time-consuming, because it needs to be retrained for every new clinical scenario. The main goal of UDA is to enable the adaptation to new domains for better generalization by matching the marginal Huang et al. [2006], Sugiyama et al. [2007], Pan et al. [2010], Gong et al. [2013] or the conditional distributions Zhang et al. [2013], Courty et al. [2017] of the labeled source and unlabeled target domains. As dearth of labeled data is the most prominent issue in the medical field, UDA methods gained a lot of attention especially in medical image analysis Guan and Liu [2022]. Owing to advantages of UDA- over SDA methods, most of the existing DA research is focused on UDA. To enable adaptation from source domain to target domain, UDA methods have to meet two important criteria, namely transferability and discriminability Chen et al. [2019]. The transferability of feature representations from source to target is the primary indicator for the performance of the model. Apart from this, the other key indicator is the ability to discriminate between the classes present in the domains. There are mainly two strategies to align feature distributions across domains: Moment matching and adversarial training Jin et al. [2020].

Moment matching methods aim to decrease the distribution discrepancy between the source and the target domain. This is achieved by matching the first/second order moments (as mean and covariance) of the activation distributions that are unique to each domain in the hidden activation space Zellinger et al. [2017]. Multiple UDA methods have been developed based on moment matching, including Deep Adaptation Networks (*DAN*) Long et al. [2015] which utilizes Maximum Mean Discrepancy (*MMD*). An extension of *DAN*, called Joint Adaptation Networks (*JAN*) Long et al. [2017] has also been established. Apart from that, Correlation Alignment (*Deep-CORAL*) Sun and Saenko [2016] is based on second order statistics of both the distributions. Another approach is *CMD* Zellinger et al. [2017], which defines a new distance function based on probability distributions by moment sequences. Methods based on divergence are typically not very complicated, easier to train and do not require a lot of hyperparameter tuning for optimization. Additionally, they are computation efficient and are not in necessity of large datasets Zhao et al. [2022]. However, the disadvantage of these types of methods is that they cannot be reliably used to achieve good performances on large datasets with more complex and diverse images. Also, they cannot be applied to other computer vision tasks, as semantic segmentation, because they do learn image-level, not pixel-level representations.

Adversarial training methods for domain adaptation learn domain-invariant features. For this, a domain discriminator is trained to differentiate between the source and the target domain by minimizing the classification error. At the same time, the feature representations learned by the classifier try to confuse the discriminator. One of the well-studied and most used adversarial methods is the Domain Adversarial Neural Network (*DANN*) Ganin and Lempitsky [2015]. Apart from *DANN*, there are other adversarial methods like Adversarial Discriminative Domain Adaptation (*ADDA*) Tzeng et al. [2017] and Maximum Classifier Discrepancy (*MCD*) Saito et al. [2018] which are developed as an extension to the *DANN* approach. Typically, adversarial methods achieve better adaptations than moment matching methods and are the more dominant method Xu et al. [2019]. They are very good in enhancing transferability of representations. Additionally, they have good computational efficiency and work across different kinds of datasets Zhao et al. [2022]. Discriminative approaches are able to adapt well on larger domain shifts Tzeng et al. [2017]. The disadvantage is that it can be difficult to optimize them. Also, in some cases they may perform poorly on small datasets, because these methods rely on the convergence of a min-max game. When having multimodal feature distributions it can be challenging for adversarial methods to adapt feature representations only Goodfellow et al. [2014], Arjovsky and Bottou [2017], Long et al. [2018]. The discriminability of the learned representation happens only by minimizing the classification error on the source domain Chen et al. [2019]. It cannot be guaranteed that the distributions are identical, even if the confusion of the discriminator was fully achieved Arora et al. [2017], Long et al. [2018].

There exist also **extensions to adversarial methods**, e.g. Batch Spectral Penalization (*BSP*) Chen et al. [2019], which can be used standalone or as a regularizer to another domain adaptation method. Also Minimum Class Confusion (*MCC*) Jin et al. [2020] can be used as a standalone adaptation method or additionally as a regularizer. The advantage of *MCC* over *BSP* is, that *MCC* as a regularizer is not limited to adversarial methods.

Besides, there is also extensive research in the direction of **adversarial generative methods** which are based on GANs. They include a generator to create virtual images, while a discriminator tries to differentiate between real and generated images Goodfellow et al. [2014]. The research in the area of conditional GANs Mirza and Osindero [2014] led to the development of methods like Conditional Adversarial Domain Adaptation (*CDAN*) Long et al. [2018]. Although adversarial generative adaptation methods usually achieve good performances, they require largely scaled data for the generator to be trained properly. Furthermore, these methods need more computational resources, as well as

hyperparameter tuning, which makes the optimization process more complex Zhao et al. [2022]. Additionally, GANs show attractive visualizations, but they can be limited to small shifts Tzeng et al. [2017].

Due to the growing demand in adapting neural networks to unseen domains, there are other popular methods like Unsupervised Image-to-Image Translation Networks (*UNIT*) Liu et al. [2017], Generate to Adapt (*GTA*) Sankaranarayanan et al. [2018], Cycle-Consistent Adversarial Domain Adaptation (*CyCADA*) Hoffman et al. [2018] and Adaptive Feature Norm (*AFN*) Xu et al. [2019].

It is important to note that this area of research is rapidly growing and new domain adaptation methods are emerging in a variety of fields, ranging from computer vision, natural language processing, video analysis to robotics. Their use-case is also not just limited to image classification tasks, but is extended to semantic segmentation, face recognition, object identification, image-to-image translation, person re-identification and image captioning among others Wang and Deng [2018]. Domain adaptation is also commonly used in medical image analysis. The leading application area of visual domain adaptation in medicine are brain images Guan and Liu [2022], while there is also research on lungs, hearts, breasts, eyes and abdomen. Mostly, these applications use histological or microscopical images.

We have noticed that there is limited work applying DA to dermoscopic images. Gu et al., Gu et al. [2020] developed a two-step progressive adaptation method for task specific skin cancer classification. In their approach, they first trained a CNN on ImageNet and further fine-tuned it on an intermediate skin cancer dataset, before fine-tuning it again on another skin cancer dataset. Apart from that, Ahn et al., Ahn et al. [2020] used a similar approach of training the model initially on ImageNet and fine-tuning it on medical images. They used context-based feature augmentation which uses additional information about the images. They experimented with medical image modality classification, a tuberculosis dataset, as well as with skin cancer datasets.

Abbreviation	Origin	Biological factors	Melanoma amount	Nevus amount	Total target size
H	HAM	Age >30, Loc. = Body (default)	465 (10%)	4234 (90%)	4699
HA	HAM	Age ≤ 30, Loc. = Body	25 (4%)	532 (96%)	557
HLH	HAM	Age >30, Loc. = Head/Neck	99 (45%)	121 (55%)	220
HLP	HAM	Age >30, Loc. = Palms/Soles	15 (7%)	203 (93%)	218
B	BCN	Age >30, Loc. = Body (default)	1918 (41%)	2721 (59%)	4639
BA	BCN	Age ≤ 30, Loc. = Body	71 (8%)	808 (92%)	879
BLH	BCN	Age >30, Loc. = Head/Neck	612 (66%)	320 (34%)	932
BLP	BCN	Age >30, Loc. = Palms/Soles	192 (65%)	105 (35%)	297
M	MSK	Age >30, Loc. = Body (default)	565 (31%)	1282 (69%)	1847
MA	MSK	Age ≤ 30, Loc. = Body	37 (8%)	427 (92%)	464
MLH	MSK	Age >30, Loc. = Head/Neck	175 (60%)	117 (40%)	292

Table 1: Overview of the datasets used for our benchmark including dataset sizes and class distributions. H represents our source dataset. All following datasets are domain shifted datasets with respect to H.

UDA methods are typically compared against each other when a new method is proposed. In that comparison the works mostly focus on performance comparisons with respect to other state-of-the-art methods. Most of the UDA methods are evaluated on well-studied datasets like ImageNet, MNIST and Office-31, whereas their performance on other datasets is expected to change based on the available data and the domains present in them. Even these benchmark datasets are not analyzed for artefacts and duplicates present within the dataset. Ringwald et al. Ringwald and Stiefelhagen [2021] analyzed frequently used UDA datasets and studied the systematic problems with regard to dataset setup and ambiguities. They established a clean Office-31 dataset for UDA algorithm comparisons. Hence, to verify the actual efficiency of the UDA methods, it is essential to study their performance on other, more real-world related datasets, as well. Peng et al., Peng et al. [2018] introduced a benchmark dataset to evaluate the performance of UDA methods. They estimate the performance of the domain adaptation models to transfer knowledge from synthetic to real data. Also, Nagananda et al., Nagananda et al. [2021] compared UDA methods on publicly available aerial datasets. In the medical field, Saat et al. Saat et al. [2022] proposed a benchmark for UDA methods on brain Magnetic Resonance Imaging (MRI) - an image segmentation task. In their work, they compared UDA methods and evaluated the performance with respect to their baseline model. The source domain consists of MRI scans from multiple centers and different scanners. Whereas the target domain consists of MRI scans from a different dataset from a single center. We noticed that there is no extensive work on benchmarking UDA methods in particular for dermoscopic skin cancer image classification.

3 Materials and Methods

3.1 Datasets

Even though some recent works used image datasets from skin lesions like MoleMap, HAM10k and ISIC Guan and Liu [2022] for their adaptation tasks, there is no study evaluating the actual and total domains present in these datasets or developing and evaluating public dermoscopic datasets particularly for domain adaptation techniques [Saat et al., 2022]. To overcome this limitation, we grouped and quantified potential technical and biological shifts in our previous work [Fogelberg et al., 2023] to obtain domain shifted dermoscopic datasets². Table 1 provides a summary of the domains observed in the dermoscopic datasets.

As we are using unsupervised approaches, the source domain is labeled and these labels are used for the classification at the end. Hence, it is essential to have a dataset that can be divided into train and test without data leakage, which is not always straightforward for dermatology datasets due to duplicated lesion images. Apart from that, in domain adaptation works, the methods are evaluated from one domain to another (domain A to domain B) and are also tested in the opposite direction (domain B to domain A) Ganin and Lempitsky [2015]. However, recent works stated that the performance of UDA methods is negatively affected by poor data quality and duplicates in the datasets Ringwald and Stiefelhagen [2021]. This can be a difficulty when using the publicly available ISIC archive images as they contain duplicates which are not necessarily marked as such Cassidy et al. [2022].

We chose a representative and large subset of HAM, dataset H (Table 1), as our only source domain for the adaptation process. For this, we used the lesion ID’s present in HAM10k to remove the duplicates in the dataset [Tschandl et al., 2018]. Therefore, the adaptation was done in one direction only, using sub-datasets HA , HLH , HLP , as well as BCN20k [Combalia et al., 2019] and MSK [Cassidy et al., 2022] datasets exclusively as target domains.

3.2 UDA Methods

Overall, we focus on single-source, single-target, homogeneous adaptation without target labels. This means that there is one fully labeled source domain and one unlabeled target domain within the same modality, and that the source and target domains share the same classes.

We selected eight state-of-the-art UDA methods (Table 2), which were selected based on different types of UDA methods, computational efficiency and a good performance on different established datasets.

UDA method	Type
DAN Ganin and Lempitsky [2015]	Moment matching
JAN Long et al. [2017]	Moment matching
DANN Ganin and Lempitsky [2015]	Adversarial training
ADDA Tzeng et al. [2017]	Adversarial training
BSP Chen et al. [2019]	Extension of adversarial
MCC Jin et al. [2020]	Extension of adversarial
CDAN Long et al. [2018]	Adversarial generative
AFN Xu et al. [2019]	Other

Table 2: Our selection of eight state-of-the-art UDA methods for the benchmark study. The methods are of different types of strategies.

3.3 Experimental setup

It is difficult to decide which UDA method is generally better compared to others in terms of design or performance. The key characteristic that determines the strength of a UDA method is its ability to transfer feature representations from a source- to a target domain. For this reason, we compare all UDA results to our unadapted baseline method (Src) trained on source dataset H , which is a basic ResNet50 model He et al. [2016] pretrained on ImageNet. The other performance characteristic is the discriminability between the classes within domains. We evaluate how well the model is able to discriminate between melanoma and nevus in our binary classification task. For this we follow standard evaluation protocols for unsupervised domain adaptation Ganin and Lempitsky [2015], Long et al. [2017]. For all experiments we used an initial learning rate (LR) of 0.01 with a weight decay of $1e-3$ and a LR-decay 0.75. The used momentum was 0.9 and gamma was 0.001. We set the epochs to 20 and the batch size to 16. The comparison

²https://gitlab.com/dlr-dw/isic_download

		Domain shifted dataset									
		HA	HLH	HLP	B	BA	BLH	BLP	M	MA	MLH
Mel (%)		4	45	7	41	8	66	65	31	8	60
(UDA) method	Src	0.14±0.02	0.69±0.04	0.37±0.15	0.57±0.02	0.19±0.06	0.73±0.03	0.77±0.05	0.34±0.01	0.15±0.04	0.68±0.03
	DAN	0.12±0.02	0.77±0.02	0.47±0.14	0.60±0.04	0.20±0.02	0.78±0.01	0.83±0.03	0.37±0.03	0.13±0.03	0.69±0.03
	JAN	0.15±0.04	0.82±0.05	0.56±0.08	0.72±0.02	0.34±0.02	0.85±0.02	0.82±0.03	0.44±0.03	0.14±0.01	0.73±0.03
	DANN	0.17±0.01	0.81±0.04	0.55±0.07	0.74±0.02	0.32±0.03	0.85±0.01	0.84±0.01	0.44±0.01	0.18±0.04	0.72±0.02
	ADDA	0.18±0.06	0.81±0.02	0.55±0.03	0.74±0.01	0.36±0.03	0.87±0.01	0.83±0.02	0.44±0.02	0.17±0.03	0.73±0.03
	CDAN	0.14±0.02	0.82±0.03	0.54±0.06	0.73±0.02	0.33±0.02	0.85±0.01	0.84±0.02	0.47±0.02	0.14±0.01	0.73±0.02
	BSP	0.16±0.03	0.82±0.02	0.65±0.04	0.75±0.01	0.34±0.05	0.86±0.01	0.83±0.02	0.46±0.02	0.17±0.03	0.73±0.01
	AFN	0.11±0.02	0.83±0.02	0.57±0.13	0.73±0.01	0.35±0.03	0.84±0.01	0.86±0.02	0.43±0.02	0.16±0.02	0.71±0.02
	MCC	0.15±0.04	0.83±0.07	0.57±0.05	0.69±0.02	0.30±0.08	0.83±0.01	0.81±0.04	0.41±0.02	0.14±0.03	0.71±0.03

Table 3: Comparison of AUPRC results across different datasets and UDA methods. The columns represent the domain shifted target datasets for the source dataset H (not listed here). Each row represents the results for a particular UDA method, with the first row indicating the results for the unadapted baseline method (Src). The best-performing UDA method for each dataset is highlighted in bold. The percentage for each dataset shows the ratio of melanoma in that dataset, which serves as the baseline for AUPRC. The source dataset H contains only 10% melanoma.

is based on an existing repository³ which already implemented a variety of methods. It is open-source and has been established on multiple popular datasets, e.g. MNIST, Office-31 and DomainNet Jiang et al. [2022, 2020]. We modified the library for our classification on dermoscopic images.

In a typical dermoscopic dataset, the presence of melanoma, in comparison to nevus images, is very low, as can be seen in Table 1. In our analysis, we consider melanoma as the positive and nevus as the negative class. When it comes to a clinical translation of a skin lesion diagnostic system, both, True Positives and True Negatives are considered very important. Therefore, we focused on AUROC and AUPRC as evaluation metrics. The advantage of these two metrics is that they are both threshold-free. That means, that they can provide an overview of the performance range with different dataset-splits into positively and negatively predicted classes Saito and Rehmsmeier [2015]. Also Zhang et al. Zhang et al. [2022b] used AUROC and AUPRC for the evaluation of their domain adaptation results in a recent work.

AUROC as a standalone metric can be misleading in imbalanced tasks, because the score can be better than random guessing (baseline=0.5), but still misclassify the minority class. On the contrary, AUPRC is tailored for such imbalanced cases, but may mislead in balanced cases or where the negatives are rare. When using only AUPRC, it can be difficult to compare results across datasets with different class ratios and dataset sizes. The reason for this is the varying baseline of this metric, as it is dependent on the ratio of the positive class. Therefore, we computed both metrics, while also focusing on the AUPRC improvement (in %) compared to the unadapted baseline method (Src), as suggested by Zhang et al. [Zhang et al., 2022a]. With this approach, the results can be compared across methods and datasets equally.

For the experiments, we included a weighted random sampler to maintain equal class ratios per batch during model training. We also adopted five-fold cross validation to use all images of the available datasets. From each fold we selected the best epoch (out of 20) and averaged the results. Additionally, we ran the experiments with five seeds to observe the variability of the results over different runs. For the end results we averaged the values over five seeds. The seeding makes the performance results more robust and that way shows more realistic values.

4 Results and Discussion

If a UDA method performs well on one dataset, it does not guarantee similar performance on other datasets. As discussed in Section 3, we have selected 8 state-of-the-art UDA methods to evaluate the performance on the domains present in our 11 dermoscopic datasets. We compared all adaptation methods with our non-adapted baseline approach.

³<https://github.com/thuml/Transfer-Learning-Library>

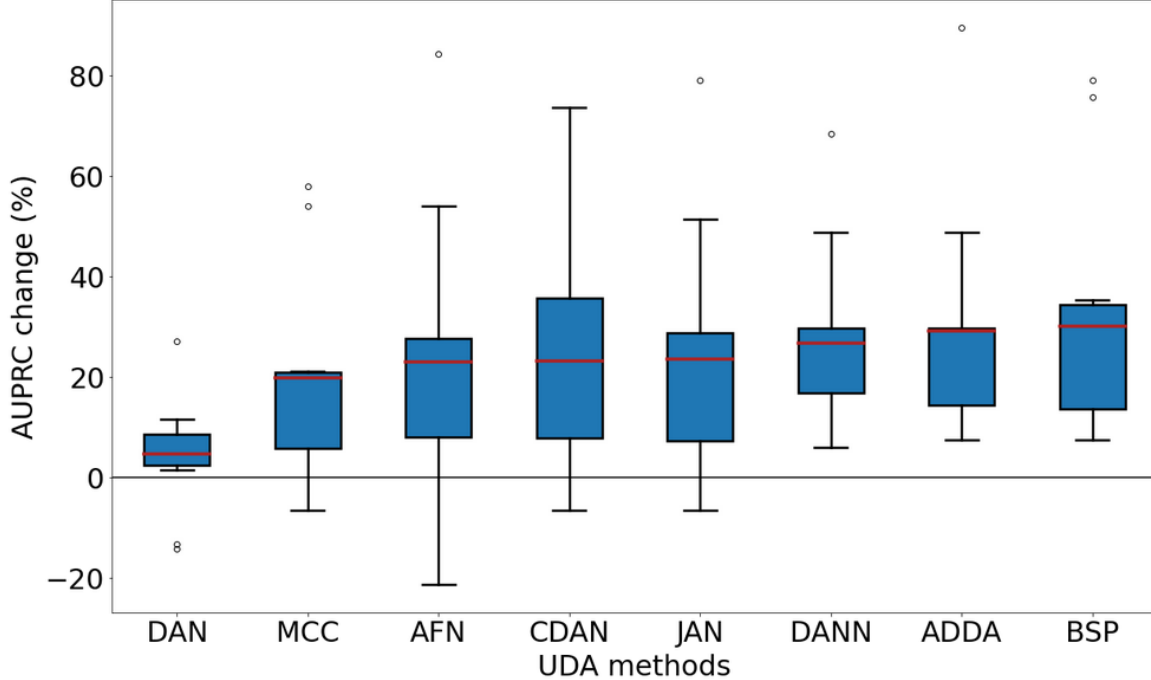


Figure 1: Comparison of UDA methods with respect to AUPRC change. The red line represents the mean (of the performance on all datasets) and the black dots are outliers. The black line shows the baseline at 0% performance improvement. The performance improvement was calculated over five seeds and averaged over 10 datasets. The UDA methods are ordered in the increasing order of the mean AUPRC change on the x-axis. The numbers in the brackets (x-axis) represent for how many datasets out of 10 this particular method improved the performance.

4.1 Benchmarking UDA methods on dermoscopic datasets

As stated in Subsection 3.3, we computed AUROC and AUPRC scores for different datasets and methods, which can be seen in Table 1 and Table 3, respectively. To provide a better understanding of our comparison and to demonstrate the quantified changes compared to *Src* method, we also looked at the AUROC- (Table 2) and AUPRC (Table 3) improvement (in %). In these tables, negative values, which indicate performance degradation after domain adaptation, occur rarely.

Our results indicate, that all selected UDA methods achieve a performance improvement (in %) compared to *Src* method over most available domain shifted datasets (Figure 1). *BSP*, *ADDA* and *DANN*, which are all adversarial types of techniques, achieve the largest performance improvement. According to our results, these three UDA methods were able to improve the performance of 10 out of 10 domain shifted dermoscopic datasets. The moment matching method *DAN* did not exhibit an improvement in performance overall.

The performance change (in %) of each individual domain shifted dataset per method is represented in Figure 2. For this overview, we combine performance change, melanoma ratio and target dataset size in one figure. While the performance is demonstrated in the upper point plot, the melanoma ratio per dataset can be observed in the lower illustration. In both sub-figures the domain shifted datasets on the x-axis are ordered by target dataset size in an ascending order from left to right. The largest improvements are achieved on dataset *BA* using either *ADDA* or *AFN* as the UDA method. However, although *BA* has the highest improvement, it has also a high variance between the methods' results, which ranges from 5.26% to 89.47%. All UDA methods, except for *DAN*, achieved maximum performance improvement at least for one dataset, as shown in Table 3. It is also noteworthy that the *MLH* dataset posed the greatest challenge for adaptation, as all UDA methods seem to encounter difficulties with it (Figure 2).

4.2 Influential factors on the performance improvement

Our analysis revealed that the amount of melanoma images in the target datasets affects the performance of UDA methods, as demonstrated in Table 3 and Figure 2. Several datasets, including *HA*, *HLP*, *MA*, and *BA*, have a low

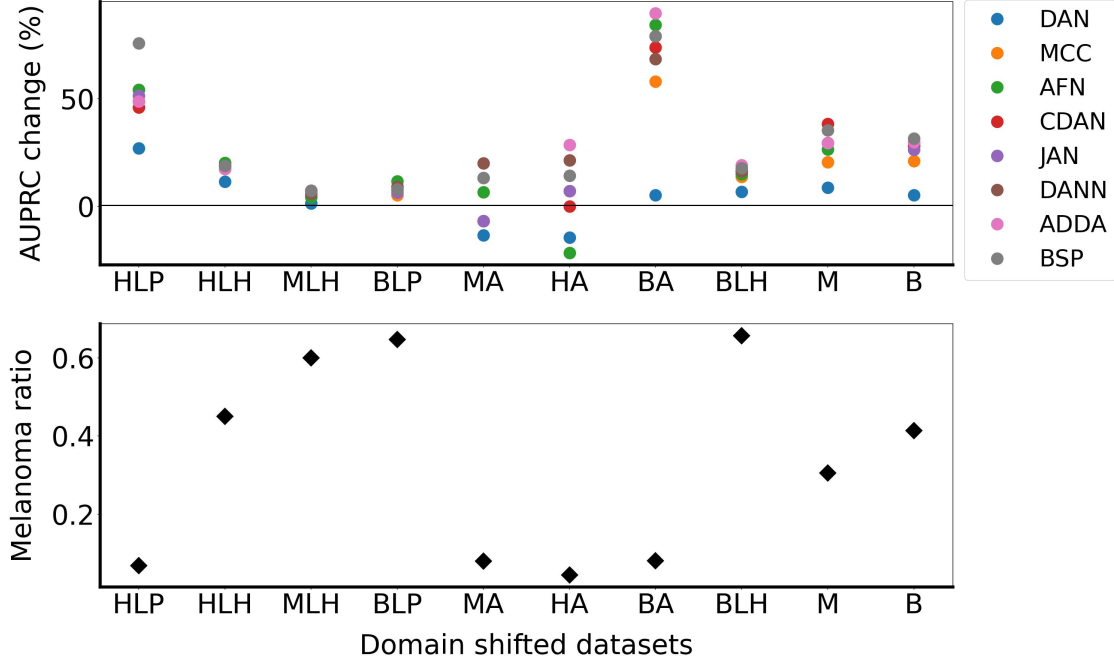


Figure 2: Change in AUPRC (in %) with respect to the unadapted baseline model (*Src*). Individual UDA methods (color-coded) are illustrated across all domain shifted datasets (x-axis). The upper panel of the figure shows the AUPRC change (in %). The black line at 0 on the y-axis highlights the methods which show a performance degradation or no improvement (w.r.t the unadapted baseline method). The lower panel shows the melanoma ratio for each dataset. The datasets on the x-axis are ordered by total target size in an ascending manner.

number of melanoma cases and also represent larger disparities between the results of all UDA methods (Table 3). Datasets *HLH*, *B* and *M* have a more balanced distribution between both classes (Table 1). Adversarial methods and their extensions appear to perform better for such imbalanced datasets. For instance, *ADDA* is the most effective UDA method for dataset *HA*, which has the lowest melanoma sample size of 4%. On the other hand, some datasets such as *BLP*, *BLH*, and *MLH* are dominated by melanoma cases and therefore all methods show similar improvement in AUPRC scores. Although no improvement can be detected from the unadapted baseline, we observe that most methods agree with each other when it comes to datasets with a high melanoma ratio (Figure 2). It is worth noting that *MA*, *HA*, and *BA* datasets contain images of skin lesions from patients below the age of 30. These datasets include both, young patients and children, as we have previously noted in our work Fogelberg et al. [2023]. Diagnosing melanoma in children is a unique challenge in clinical diagnosis, as they do not show typical ABCDE features [Duarte et al., 2021] used to identify melanomas in adults due to their different appearance [Scope et al., 2016]. This may result in a lower performance improvement after adaptation.

To achieve performance improvements in UDA methods, it is necessary to have a large dataset available for the training process of the adaptation method Motiian et al. [2017]. As shown in Table 3 and Figure 2, for the larger datasets *M* and *B*, most of the methods (except for *DAN*) showed higher improvement in performance compared to other datasets. Interestingly, these two datasets have a balanced class distribution. However, the overall performance is also linked to the melanoma ratio in the dataset. An exception to this observation is dataset *HLP* where most methods show agreement despite the small dataset size and low melanoma ratio. We assume this is because of the relative similarity of the target dataset to the source dataset (*H*). In our previous analysis Fogelberg et al. [2023], we found that *HLP* is one of the most similar datasets to *H* in terms of melanoma images, as measured by cosine similarity and JS-divergence. It is also worth noting that for this dataset, the variation between the least performing *DAN* and the best performing *BSP* method is also high.

Regarding the AUROC and AUPRC metrics, it appears that adversarial methods and their extensions generally outperform moment matching methods, with the exception of *JAN* for the *MLH* dataset in terms of AUPRC score. This finding is consistent with existing literature indicating that adversarial methods tend to perform better than moment matching methods Xu et al. [2019].

In summary, there are various factors that contribute to the performance of UDA methods, such as melanoma ratio, target size, and how similar or dissimilar datasets are with respect to the source dataset H . However, it remains unclear which factor or combination of factors has the greatest influence on performance improvement with UDA. Therefore, it is essential to continue investigating and exploring these factors to better understand their impact on UDA performance.

4.3 Performance of UDA methods on non-dermoscopic datasets

Another reason for the usage of AUROC for evaluation is that various works on UDA methods compare their results either with AUROC or accuracy. In particular in the medical field it is common practice to compare methods based on AUROC scores Purushotham et al. [2017], Zhou et al. [2022], Feng et al. [2023]. Most of the domain adaptation studies use accuracy as their metric for comparisons of methods, but none of these studies discuss the possible imbalance in their datasets.

Typical datasets used for domain adaptation tasks are, for instance, Digits or Office-31. These images are easier to adapt to and differ a lot more than dermoscopic images do. Moreover, benchmark datasets for UDA are typically large, have almost balanced classes and the classification ability can even be validated by non-expert humans. On the contrary, dermoscopic images look very similar, making the task not only difficult for medical experts, but also for the neural network. Backgrounds can contain complex structures, which are artefacts used by the neural networks for training, such as black borders, hair or skin colour.

When comparing all used methods, DAN performs poorly in our dermoscopic scenario, as well as in other adaptation tasks Long et al. [2015], Ganin and Lempitsky [2015], Long et al. [2017], Tzeng et al. [2017], Long et al. [2018], Chen et al. [2019], Xu et al. [2019], Jin et al. [2020]. Our selection of UDA methods are benchmarked on Office-31-, Office-Home, ImageCLEF-DA- and VisDA17-datasets. It is worth noting that not all UDA methods are compared in each work and on each of these datasets. Therefore, a fair comparison of non-dermoscopic results is not possible.

We can observe, that the adversarial UDA methods, namely *BSP* and *ADDA*, which are overall performing better in our dermoscopic scenario, also perform very well in other image classification tasks. According to the authors of Chen et al. [2019], their method *BSP* specifically boosts the performance on relatively difficult tasks, where the source domain is quite small. *ADDA* was not often compared in these works, but it is outperformed by *CDAN* in Office-31 adaptation. For all other methods, it is not possible to provide a clear order of performance improvements as they are compared on different tasks and with different methods. *DAN*, *DANN* and *JAN* are outperformed by all mentioned methods in Office-31-, ImageCLEF-DA-, Office-Home- and VisDA17-adaptation. *CDAN* is outperformed in Office-Home-, Office-31- and VisDA17-adaptation by *AFN*, *MCC* and *BSP+CDAN*.

5 Conclusion

This is the first work benchmarking UDA methods on dermoscopic datasets. In summary, our work enables the reproducibility of results and interpretation due to the utilization of publicly available dermoscopic datasets. Further, the domain shifts in between the datasets were quantified, unlike for most used benchmark datasets. Our analysis shows that all selected UDA methods from different technical approaches improve the performance for most datasets compared to the unadapted technique, although in different extents.

We have additionally conducted a comparative analysis on the dependency of the performance of UDA methods on dataset-dependent features like class imbalance and target dataset size. We have noticed that the overall performance of UDA methods depends on various combinations of factors.

Moreover, we compared how our chosen UDA methods perform for other typical benchmark adaptation tasks in comparison to our dermoscopic datasets. In general, the UDA methods that performed well on dermoscopic datasets are also the best performing methods on other non-dermoscopic tasks.

In our analysis our aim was to compare different UDA methods on the same (well-established) ResNet-50 backbone. However, the selection of the backbone has an impact on the overall performance Feng et al. [2023]. One further extension can be the comparison of different backbones and how it influences the performances. Another important future aspect is to investigate the intensity of performance degradation when reducing the target dataset size. It is worth exploring the field of few/one/zero-shot domain adaptation. Another possible area of interest is multi-source domain adaptation (multiple modalities) on dermoscopic datasets, where e.g. dermoscopic and clinical lesion images can be included. UDA could be recommended for adversarial methods, as these have consistently shown the most improvements. Ideally, the datasets should be balanced, because a low melanoma ratio was indicative of a high performance variance, thus making the applied methods riskier.

Acknowledgements

This research is funded by the *Helmholtz Artificial Intelligence Cooperation Unit* [grant number ZT-I-PF-5-066].

The Helmholtz AI funding enabled the close cooperation between DKFZ and DLR, which leads to an interdisciplinary exchange between two research groups and thereby enables the integration of novel perspectives and experiences.

References

- E. Ahn, A. Kumar, M. Fulham, D. Feng, and J. Kim. Unsupervised domain adaptation to classify medical images using zero-bias convolutional auto-encoders and context-based feature augmentation. *IEEE Transactions on Medical Imaging*, 39(7):2385–2394, jul 2020. doi:10.1109/tmi.2020.2971258. URL <https://doi.org/10.1109/tmi.2020.2971258>.
- M. Arjovsky and L. Bottou. Towards principled methods for training generative adversarial networks. In *International Conference on Learning Representations*, 2017. URL https://openreview.net/forum?id=Hk4_qw5xe.
- S. Arora, R. Ge, Y. Liang, T. Ma, and Y. Zhang. Generalization and equilibrium in generative adversarial nets (GANs). In D. Precup and Y. W. Teh, editors, *Proceedings of the 34th International Conference on Machine Learning*, volume 70 of *Proceedings of Machine Learning Research*, pages 224–232. PMLR, 06–11 Aug 2017. URL <https://proceedings.mlr.press/v70/arora17a.html>.
- S. Ben-David, J. Blitzer, K. Crammer, A. Kulesza, F. Pereira, and J. W. Vaughan. A theory of learning from different domains. *Machine Learning*, 79(1-2):151–175, oct 2009. doi:10.1007/s10994-009-5152-4. URL <https://doi.org/10.1007/s10994-009-5152-4>.
- B. Cassidy, C. Kendrick, A. Brodzicki, J. Jaworek-Korjakowska, and M. H. Yap. Analysis of the isic image datasets: usage, benchmarks and recommendations. *Medical Image Analysis*, 75:102305, 2022. doi:10.1016/j.media.2021.102305. URL <https://doi.org/10.1016/j.media.2021.102305>.
- X. Chen, S. Wang, M. Long, and J. Wang. Transferability vs. discriminability: Batch spectral penalization for adversarial domain adaptation. In K. Chaudhuri and R. Salakhutdinov, editors, *Proceedings of the 36th International Conference on Machine Learning*, volume 97 of *Proceedings of Machine Learning Research*, pages 1081–1090. PMLR, 09–15 Jun 2019. URL <https://proceedings.mlr.press/v97/chen19i.html>.
- M. Combalia, N. C. Codella, V. Rotemberg, B. Helba, V. Vilaplana, O. Reiter, C. Carrera, A. Barreiro, A. C. Halpern, S. Puig, et al. Bcn20000: Dermoscopic lesions in the wild. *arXiv preprint arXiv:1908.02288*, 2019. doi:10.48550/arXiv.1908.02288. URL <https://doi.org/10.48550/arXiv.1908.02288>.
- N. Courty, R. Flamary, A. Habrard, and A. Rakotomamonjy. Joint distribution optimal transportation for domain adaptation. *Advances in neural information processing systems*, 30, 2017. doi:10.48550/arXiv.1705.08848. URL <https://doi.org/10.48550/arXiv.1705.08848>.
- A. F. Duarte, B. Sousa-Pinto, L. F. Azevedo, A. M. Barros, S. Puig, J. Malvehy, E. Haneke, and O. Correia. Clinical abcde rule for early melanoma detection. *European Journal of Dermatology*, 31(6):771–778, 2021. URL <https://doi.org/10.1684/ejd.2021.4171>.
- Y. Feng, Z. Wang, X. Xu, Y. Wang, H. Fu, S. Li, L. Zhen, X. Lei, Y. Cui, J. S. Z. Ting, Y. Ting, J. T. Zhou, Y. Liu, R. S. M. Goh, and C. H. Tan. Contrastive domain adaptation with consistency match for automated pneumonia diagnosis. *Medical Image Analysis*, 83:102664, jan 2023. doi:10.1016/j.media.2022.102664. URL <https://doi.org/10.1016/j.media.2022.102664>.
- K. Fogelberg, S. Chamarthi, R. C. Maron, J. Niebling, and T. J. Brinker. Domain shifts in dermoscopic skin cancer datasets: Evaluation of essential limitations for clinical translation. *New Biotechnology*, 76:106–117, 2023. ISSN 1871-6784. doi:<https://doi.org/10.1016/j.nbt.2023.04.006>. URL <https://www.sciencedirect.com/science/article/pii/S1871678423000213>.
- Y. Ganin and V. Lempitsky. Unsupervised domain adaptation by backpropagation. In *International conference on machine learning*, pages 1180–1189. PMLR, 2015. URL <https://dl.acm.org/doi/10.5555/3045118.3045244>.
- B. Gong, K. Grauman, and F. Sha. Connecting the dots with landmarks: Discriminatively learning domain-invariant features for unsupervised domain adaptation. In *International conference on machine learning*, pages 222–230. PMLR, 2013. doi:10.5555/3042817.3042844. URL <https://dl.acm.org/doi/10.5555/3042817.3042844>.
- I. Goodfellow, J. Pouget-Abadie, M. Mirza, B. Xu, D. Warde-Farley, S. Ozair, A. Courville, and Y. Bengio. Generative adversarial nets. In Z. Ghahramani, M. Welling, C. Cortes, N. Lawrence, and K. Weinberger, editors, *Advances in Neural Information Processing Systems*, volume 27. Curran Associates, Inc., 2014. URL <https://proceedings.neurips.cc/paper/2014/file/5ca3e9b122f61f8f06494c97b1afccf3-Paper.pdf>.

- Y. Gu, Z. Ge, C. P. Bonnington, and J. Zhou. Progressive transfer learning and adversarial domain adaptation for cross-domain skin disease classification. *IEEE Journal of Biomedical and Health Informatics*, 24(5):1379–1393, may 2020. doi:10.1109/jbhi.2019.2942429. URL <https://doi.org/10.1109/jbhi.2019.2942429>.
- H. Guan and M. Liu. Domain adaptation for medical image analysis: A survey. *IEEE Transactions on Biomedical Engineering*, 69(3):1173–1185, mar 2022. doi:10.1109/tbme.2021.3117407. URL <https://doi.org/10.1109/tbme.2021.3117407>.
- L. L. Guo, S. R. Pfohl, J. Fries, A. Johnson, J. Posada, C. Aftandilian, N. Shah, and L. Sung. Evaluation of domain generalization and adaptation on improving model robustness to temporal dataset shift in clinical medicine. jun 2021. doi:10.1101/2021.06.17.21259092. URL <https://doi.org/10.1101/2021.06.17.21259092>.
- K. He, X. Zhang, S. Ren, and J. Sun. Deep residual learning for image recognition. In *2016 IEEE Conference on Computer Vision and Pattern Recognition (CVPR)*. IEEE, jun 2016. doi:10.1109/cvpr.2016.90. URL <https://doi.org/10.1109/cvpr.2016.90>.
- J. Hoffman, E. Tzeng, T. Park, J.-Y. Zhu, P. Isola, K. Saenko, A. Efros, and T. Darrell. Cycada: Cycle-consistent adversarial domain adaptation. In *International conference on machine learning*, pages 1989–1998. Pmlr, 2018. URL <http://proceedings.mlr.press/v80/hoffman18a/hoffman18a.pdf>.
- J. Huang, A. Gretton, K. Borgwardt, B. Schölkopf, and A. Smola. Correcting sample selection bias by unlabeled data. In B. Schölkopf, J. Platt, and T. Hoffman, editors, *Advances in Neural Information Processing Systems*, volume 19. MIT Press, 2006. URL <https://proceedings.neurips.cc/paper/2006/file/a2186aa7c086b46ad4e8bf81e2a3a19b-Paper.pdf>.
- J. Jiang, B. Chen, B. Fu, and M. Long. Transfer-learning-library. <https://github.com/thuml/Transfer-Learning-Library>, 2020.
- J. Jiang, Y. Shu, J. Wang, and M. Long. Transferability in deep learning: A survey, 2022. URL <https://arxiv.org/abs/2201.05867>.
- Y. Jin, X. Wang, M. Long, and J. Wang. Minimum class confusion for versatile domain adaptation. In *Computer Vision – ECCV 2020*, pages 464–480. Springer International Publishing, 2020. doi:10.1007/978-3-030-58589-1_28. URL https://doi.org/10.1007/978-3-030-58589-1_28.
- M.-Y. Liu, T. Breuel, and J. Kautz. Unsupervised image-to-image translation networks. *arXiv e-prints*, art. arXiv:1703.00848, Mar. 2017. doi:10.48550/arXiv.1703.00848. URL <https://arxiv.org/abs/1703.00848>.
- M. Long, Y. Cao, J. Wang, and M. Jordan. Learning transferable features with deep adaptation networks. In *International conference on machine learning*, pages 97–105. PMLR, 2015. URL <https://dl.acm.org/doi/10.5555/3045118.3045130>.
- M. Long, H. Zhu, J. Wang, and M. I. Jordan. Deep transfer learning with joint adaptation networks. In *International conference on machine learning*, pages 2208–2217. PMLR, 2017. URL <https://dl.acm.org/doi/10.5555/3305890.3305909>.
- M. Long, Z. CAO, J. Wang, and M. I. Jordan. Conditional adversarial domain adaptation. In S. Bengio, H. Wallach, H. Larochelle, K. Grauman, N. Cesa-Bianchi, and R. Garnett, editors, *Advances in Neural Information Processing Systems*, volume 31. Curran Associates, Inc., 2018. URL <https://proceedings.neurips.cc/paper/2018/file/ab88b15733f543179858600245108dd8-Paper.pdf>.
- M. Mirza and S. Osindero. Conditional generative adversarial nets. *arXiv e-prints*, Nov. 2014. doi:10.48550/arXiv.1411.1784. URL <https://arxiv.org/abs/1411.1784>.
- S. Motiian, Q. Jones, S. M. Iranmanesh, and G. Doretto. Few-shot adversarial domain adaptation. In *Proceedings of the 31st International Conference on Neural Information Processing Systems, NIPS’17*, page 6673–6683, Red Hook, NY, USA, 2017. Curran Associates Inc. ISBN 9781510860964. URL <https://dl.acm.org/doi/10.5555/3295222.3295412>.
- N. Nagananda, A. M. N. Taufique, R. Madappa, C. S. Jahan, B. Minnehan, T. Rovito, and A. Savakis. Benchmarking domain adaptation methods on aerial datasets. *Sensors*, 21(23):8070, dec 2021. doi:10.3390/s21238070. URL <https://doi.org/10.3390/s21238070>.
- Y. Ovadia, E. Fertig, J. Ren, Z. Nado, D. Sculley, S. Nowozin, J. Dillon, B. Lakshminarayanan, and J. Snoek. Can you trust your model’s uncertainty? evaluating predictive uncertainty under dataset shift. In H. Wallach, H. Larochelle, A. Beygelzimer, F. d’Alché-Buc, E. Fox, and R. Garnett, editors, *Advances in Neural Information Processing Systems*, volume 32. Curran Associates, Inc., 2019. URL https://proceedings.neurips.cc/paper_files/paper/2019/file/8558cb408c1d76621371888657d2eb1d-Paper.pdf.
- S. J. Pan and Q. Yang. A survey on transfer learning. *IEEE Transactions on knowledge and data engineering*, 22(10):1345–1359, 2010. doi:10.1109/TKDE.2009.191. URL <https://doi.org/10.1109/TKDE.2009.191>.

- S. J. Pan, I. W. Tsang, J. T. Kwok, and Q. Yang. Domain adaptation via transfer component analysis. *IEEE transactions on neural networks*, 22(2):199–210, 2010. doi:10.1109/TNN.2010.2091281. URL <https://doi.org/10.1109/TNN.2010.2091281>.
- V. M. Patel, R. Gopalan, R. Li, and R. Chellappa. Visual domain adaptation: A survey of recent advances. *IEEE Signal Processing Magazine*, 32(3):53–69, may 2015. doi:10.1109/msp.2014.2347059. URL <https://doi.org/10.1109/msp.2014.2347059>.
- X. Peng, B. Usman, N. Kaushik, D. Wang, J. Hoffman, and K. Saenko. VisDA: A synthetic-to-real benchmark for visual domain adaptation. In *2018 IEEE/CVF Conference on Computer Vision and Pattern Recognition Workshops (CVPRW)*. IEEE, jun 2018. doi:10.1109/cvprw.2018.00271. URL <https://doi.org/10.1109/cvprw.2018.00271>.
- S. Purushotham, W. Carvalho, T. Nilanon, and Y. Liu. Variational recurrent adversarial deep domain adaptation. In *International Conference on Learning Representations*, 2017. URL <https://openreview.net/forum?id=rk9eAFcxg>.
- J. Quinero-Candela, M. Sugiyama, A. Schwaighofer, and N. D. Lawrence. *Dataset shift in machine learning*. MIT Press, 2008. doi:10.5555/1462129. URL <https://dl.acm.org/doi/10.5555/1462129>.
- T. Ringwald and R. Stiefelwagen. Adaptope: A modern benchmark for unsupervised domain adaptation. In *2021 IEEE Winter Conference on Applications of Computer Vision (WACV)*. IEEE, jan 2021. doi:10.1109/wacv48630.2021.00015. URL <https://doi.org/10.1109/wacv48630.2021.00015>.
- P. Saat, N. Nogovitsyn, M. Y. Hassan, M. A. Ganaie, R. Souza, and H. Hemmati. A domain adaptation benchmark for t1-weighted brain magnetic resonance image segmentation. *Frontiers in Neuroinformatics*, 16, sep 2022. doi:10.3389/fninf.2022.919779. URL <https://doi.org/10.3389/fninf.2022.919779>.
- K. Saito, K. Watanabe, Y. Ushiku, and T. Harada. Maximum classifier discrepancy for unsupervised domain adaptation. In *2018 IEEE/CVF Conference on Computer Vision and Pattern Recognition*. IEEE, jun 2018. doi:10.1109/cvpr.2018.00392. URL <https://doi.org/10.1109/cvpr.2018.00392>.
- T. Saito and M. Rehmsmeier. The precision-recall plot is more informative than the roc plot when evaluating binary classifiers on imbalanced datasets. *PloS one*, 10(3):e0118432, 2015. URL <https://doi.org/10.1371/journal.pone.0118432>.
- S. Sankaranarayanan, Y. Balaji, C. D. Castillo, and R. Chellappa. Generate to adapt: Aligning domains using generative adversarial networks. In *2018 IEEE/CVF Conference on Computer Vision and Pattern Recognition (CVPR)*, pages 8503–8512, Los Alamitos, CA, USA, jun 2018. IEEE Computer Society. doi:10.1109/CVPR.2018.00887. URL <https://doi.ieeecomputersociety.org/10.1109/CVPR.2018.00887>.
- A. Scope, M. A. Marchetti, A. A. Marghoob, S. W. Dusza, A. C. Geller, J. M. Satagopan, M. A. Weinstock, M. Berwick, and A. C. Halpern. The study of nevi in children: Principles learned and implications for melanoma diagnosis. *Journal of the American Academy of Dermatology*, 75(4):813–823, 2016. doi:10.1016/j.jaad.2016.03.027. URL <https://doi.org/10.1016/j.jaad.2016.03.027>.
- M. Sugiyama, S. Nakajima, H. Kashima, P. Buenau, and M. Kawanabe. Direct importance estimation with model selection and its application to covariate shift adaptation. In J. Platt, D. Koller, Y. Singer, and S. Roweis, editors, *Advances in Neural Information Processing Systems*, volume 20. Curran Associates, Inc., 2007. URL <https://proceedings.neurips.cc/paper/2007/file/be83ab3ecd0db773eb2dc1b0a17836a1-Paper.pdf>.
- B. Sun and K. Saenko. Deep coral: Correlation alignment for deep domain adaptation. In *Computer Vision—ECCV 2016 Workshops: Amsterdam, The Netherlands, October 8–10 and 15–16, 2016, Proceedings, Part III 14*, pages 443–450. Springer, 2016. URL https://doi.org/10.1007/978-3-319-49409-8_35.
- P. Tschandl, C. Rosendahl, and H. Kittler. The ham10000 dataset, a large collection of multi-source dermatoscopic images of common pigmented skin lesions. *Scientific data*, 5(1):1–9, 2018. doi:10.1038/sdata.2018.161. URL <https://doi.org/10.1038/sdata.2018.161>.
- E. Tzeng, J. Hoffman, K. Saenko, and T. Darrell. Adversarial discriminative domain adaptation. In *2017 IEEE Conference on Computer Vision and Pattern Recognition (CVPR)*. IEEE, jul 2017. doi:10.1109/cvpr.2017.316. URL <https://doi.org/10.1109/cvpr.2017.316>.
- J. Wang, C. Lan, C. Liu, Y. Ouyang, and T. Qin. Generalizing to unseen domains: A survey on domain generalization. In *Proceedings of the Thirtieth International Joint Conference on Artificial Intelligence*. International Joint Conferences on Artificial Intelligence Organization, aug 2021. doi:10.24963/ijcai.2021/628. URL <https://doi.org/10.24963/ijcai.2021/628>.
- M. Wang and W. Deng. Deep visual domain adaptation: A survey. *Neurocomputing*, 312:135–153, oct 2018. doi:10.1016/j.neucom.2018.05.083. URL <https://doi.org/10.1016/j.neucom.2018.05.083>.

- R. Xu, G. Li, J. Yang, and L. Lin. Larger norm more transferable: An adaptive feature norm approach for unsupervised domain adaptation. In *2019 IEEE/CVF International Conference on Computer Vision (ICCV)*. IEEE, oct 2019. doi:10.1109/iccv.2019.00151. URL <https://doi.org/10.1109/iccv.2019.00151>.
- H. Yao, Y. Wang, S. Li, L. Zhang, W. Liang, J. Zou, and C. Finn. Improving out-of-distribution robustness via selective augmentation. In *International Conference on Machine Learning*, pages 25407–25437. PMLR, 2022. URL <https://openreview.net/forum?id=zXne1klXIQ>.
- J. Yosinski, J. Clune, Y. Bengio, and H. Lipson. How transferable are features in deep neural networks? *Advances in neural information processing systems*, 27, 2014. doi:10.48550/arXiv.1411.1792. URL <https://doi.org/10.48550/arXiv.1411.1792>.
- W. Zellinger, T. Grubinger, E. Lughofer, T. Natschläger, and S. Saminger-Platz. Central moment discrepancy (cmd) for domain-invariant representation learning. *arXiv preprint arXiv:1702.08811*, 2017. doi:10.48550/arXiv.1702.08811. URL <https://arxiv.org/abs/1702.08811>.
- K. Zhang, B. Schölkopf, K. Muandet, and Z. Wang. Domain adaptation under target and conditional shift. In S. Dasgupta and D. McAllester, editors, *Proceedings of the 30th International Conference on Machine Learning*, volume 28 of *Proceedings of Machine Learning Research*, pages 819–827, Atlanta, Georgia, USA, 17–19 Jun 2013. PMLR. URL <https://proceedings.mlr.press/v28/zhang13d.html>.
- L. Zhang, P. Germain, Y. Kessaci, and C. Biernacki. Interpretable domain adaptation for hidden subdomain alignment in the context of pre-trained source models. *Proceedings of the AAAI Conference on Artificial Intelligence*, 36(8): 9057–9065, jun 2022a. doi:10.1609/aaai.v36i8.20890. URL <https://doi.org/10.1609/aaai.v36i8.20890>.
- T. Zhang, M. Chen, and A. A. Bui. AdaDiag: Adversarial domain adaptation of diagnostic prediction with clinical event sequences. *Journal of Biomedical Informatics*, 134:104168, oct 2022b. doi:10.1016/j.jbi.2022.104168. URL <https://doi.org/10.1016/j.jbi.2022.104168>.
- Y. Zhang. A survey of unsupervised domain adaptation for visual recognition. *arXiv preprint arXiv:2112.06745*, 2021. URL <https://arxiv.org/abs/2112.06745>.
- S. Zhao, X. Yue, S. Zhang, B. Li, H. Zhao, B. Wu, R. Krishna, J. E. Gonzalez, A. L. Sangiovanni-Vincentelli, S. A. Seshia, and K. Keutzer. A review of single-source deep unsupervised visual domain adaptation. *IEEE Transactions on Neural Networks and Learning Systems*, 33(2):473–493, feb 2022. doi:10.1109/tnnls.2020.3028503. URL <https://doi.org/10.1109/tnnls.2020.3028503>.
- J. Zhou, B. Jing, Z. Wang, H. Xin, and H. Tong. SODA: Detecting COVID-19 in chest x-rays with semi-supervised open set domain adaptation. *IEEE/ACM Transactions on Computational Biology and Bioinformatics*, 19(5):2605–2612, sep 2022. doi:10.1109/tcbb.2021.3066331. URL <https://doi.org/10.1109/tcbb.2021.3066331>.

A

		Domain shifted dataset									
		HA	HLH	HLP	B	BA	BLH	BLP	M	MA	MLH
(UDA) method	Src	0.65±0.04	0.74±0.05	0.82±0.08	0.65±0.01	0.58±0.05	0.61±0.03	0.62±0.07	0.51±0.01	0.60±0.05	0.57±0.03
	DAN	0.64±0.06	0.79±0.02	0.85±0.06	0.67±0.02	0.59±0.02	0.65±0.02	0.70±0.06	0.52±0.02	0.52±0.05	0.59±0.04
	JAN	0.71±0.04	0.85±0.03	0.92±0.02	0.76±0.01	0.69±0.01	0.74±0.02	0.69±0.04	0.62±0.03	0.55±0.06	0.61±0.02
	DANN	0.73±0.03	0.84±0.03	0.91±0.03	0.78±0.01	0.67±0.02	0.75±0.01	0.72±0.02	0.62±0.01	0.60±0.03	0.62±0.03
	ADDA	0.74±0.06	0.84±0.01	0.92±0.01	0.78±0.01	0.68±0.04	0.77±0.01	0.70±0.03	0.62±0.01	0.59±0.03	0.63±0.03
	CDAN	0.71±0.05	0.85±0.01	0.90±0.03	0.77±0.01	0.68±0.03	0.75±0.02	0.71±0.02	0.64±0.02	0.56±0.02	0.62±0.03
	BSP	0.72±0.03	0.84±0.01	0.94±0.02	0.78±0.01	0.70±0.04	0.75±0.02	0.71±0.02	0.64±0.02	0.56±0.02	0.62±0.02
	AFN	0.67±0.03	0.85±0.02	0.92±0.05	0.76±0.01	0.66±0.01	0.73±0.01	0.73±0.03	0.60±0.01	0.55±0.02	0.60±0.02
	MCC	0.70±0.01	0.87±0.03	0.94±0.02	0.76±0.01	0.68±0.03	0.73±0.01	0.70±0.04	0.61±0.03	0.58±0.08	0.59±0.02

Table 1: Comparison of AUROC results across different datasets and UDA methods. The columns represent the domain shifted target datasets for the source dataset H (not listed here). Each row represents the results for a particular UDA method, with the first row indicating the results for the unadapted baseline method (Src). The best-performing UDA method for each dataset is highlighted in bold.

		Domain shifted dataset									
		HA	HLH	HLP	B	BA	BLH	BLP	M	MA	MLH
UDA method	DAN	-1.54	6.76	3.66	3.08	1.72	6.56	12.9	1.96	-13.33	3.51
	JAN	9.23	14.86	12.20	16.92	18.97	21.31	11.29	21.57	-8.33	7.02
	DANN	12.31	13.51	10.98	20.00	15.52	22.95	16.13	21.57	0	8.77
	ADDA	13.85	13.51	12.20	20.00	17.24	26.23	12.90	21.57	-1.67	10.53
	CDAN	9.23	14.86	9.76	18.46	17.24	22.95	14.52	25.49	-6.67	8.77
	BSP	10.77	13.51	14.63	20.00	20.69	22.95	14.52	25.49	-6.67	8.77
	AFN	3.08	14.86	12.20	16.92	13.79	19.67	17.74	17.65	-8.33	5.26
	MCC	7.69	17.57	14.63	16.92	17.24	19.67	12.9	19.61	-3.33	3.51

Table 2: Comparison of change in AUROC results for each UDA method with respect to the unadapted baseline method (Src) for different datasets. H is the source dataset and the target datasets are listed in columns. The rows represent the improvements (in %) for each UDA-method.

		Domain shifted dataset									
		HA	HLH	HLP	B	BA	BLH	BLP	M	MA	MLH
UDA method	DAN	-14.29	11.59	27.03	5.26	5.26	6.85	7.79	8.82	-13.33	1.47
	JAN	7.14	18.84	51.35	26.32	78.95	16.44	6.49	29.41	-6.67	7.35
	DANN	21.43	17.39	48.65	29.82	68.42	16.44	9.09	29.41	20.00	5.88
	ADDA	28.57	17.39	48.65	29.82	89.47	19.18	7.79	29.41	13.33	7.35
	CDAN	0	18.84	45.95	28.07	73.68	16.44	9.09	38.24	-6.67	7.35
	BSP	14.29	18.84	75.68	31.58	78.95	17.81	7.79	35.29	13.33	7.35
	AFN	-21.43	20.29	54.05	28.07	84.21	15.07	11.69	26.47	6.67	4.41
	MCC	7.14	20.29	54.05	21.05	57.89	13.70	5.19	20.59	-6.67	4.41

Table 3: Comparison of change in AUPRC results for each UDA method with respect to the unadapted baseline method (Src) for different datasets. H is the source dataset and the target datasets are listed in columns. The rows represent the improvements (in %) for each UDA-method.